



Reconstruction of thin films polyazomethine based on microscopic images

J. Weszka^{a,b,*}, M. Szindler^a, A. Śliwa^a, B. Hajduk^{a,b}, J. Jurusik^b

^a Division of Materials Processing Technology, Management and Computer Techniques in Materials Science, Institute of Engineering Materials and Biomaterials, Silesian University of Technology, ul. Konarskiego 18a, 44-100 Gliwice, Poland

^b Department of Physics, Center of Polymer and Carbon Materials, Polish Academy of Sciences, ul. M. Curie-Skłodowska 34, 41-819 Zabrze, Poland

* Corresponding author: E-mail address: Jan.Weszka@polsl.pl

Received 05.01.2011; published in revised form 01.03.2011

ABSTRACT

Purpose: The aim of this paper was to investigate changes in surface morphology of thin films of polyazomethine PPI. Thin films were prepared using low-temperature chemical vapor deposition (CVD) method.

Design/methodology/approach: The changes in surface topography was observed by the atomic force microscope AFM and scanning electron microscope SEM. The results of roughness have been prepared in the software WSxM NanoTec Spanish company.

Findings: Results and their analysis allow to conclude that the transporting gas, which is an important factor in technology has a significant influence on surface morphology of thin films poliazomethine PPI. Known polyazomethine electrical properties and the possibility of obtaining a uniform thin layer show that it can be good material for optoelectronic and photovoltaic application.

Practical implications: Known polyazomethine electrical properties and the possibility of obtaining a uniform thin layer show that it can be good material for optoelectronic and photovoltaic application.

Originality/value: The paper presents some researches of polyazomethine thin films deposited by low-temperature chemical vapor deposition on glass BK7.

Keywords: Polyazomethine thin film; Chemical Vapor Deposition; Atomic Force Microscope; Scanning Electron Microscope, WSxM software

Reference to this paper should be given in the following way:

J. Weszka, M. Szindler, A. Śliwa, B. Hajduk, J. Jurusik, Reconstruction of thin films polyazomethine based on microscopic images, Archives of Materials Science and Engineering 48/1 (2011) 40-48.

METHODOLOGY OF RESEARCH, ANALYSIS AND MODELLING

1. Introduction

We are used to polymers as something opposite to the metals. They insulate, they do not conduct electricity.

Yet Alan J. Heeger, Alan G. MacDiarmid and Hideki Shirakawa have changed this view with their discovery that

a polymer, polyacetylene, can be made conductive almost like a metal. Polyacetylene was already known as a black powder when in 1974 it was prepared as a silvery film by Shirakawa and co-workers from acetylene, using a *Ziegler-Natta* catalyst. But despite its metallic appearance it was not a conductor. In 1977, however, Shirakawa, MacDiarmid and Heeger discovered that oxidation with

chlorine, bromine or iodine vapour made polyacetylene films 10^9 times more conductive than they were originally. Today conductive polymers are being developed for many uses, such as corrosion inhibitors, compact capacitors, antistatic coatings, transistors, light emitting diodes or solar cells [1-3].

BBC group report says that the global market for electroactive polymers increased from 290 million pounds in 2007 to an estimated 315 million pounds in 2008 (Fig. 1) [4].

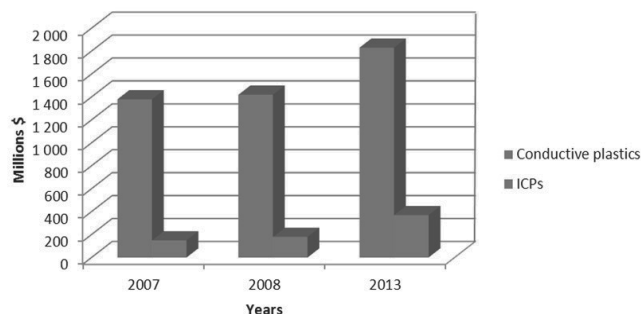


Fig. 1. Summary figure electroactive polymer market, 2007-2013 (\$ millions) [4]

A key property of a conductive polymer is the presence of conjugated double bonds along the backbone of the polymer. In conjugation, the bonds between the carbon atoms are alternately single and double [1-3].

Synthesis and characterization of conjugated polymers have attracted much attention because of academic interest and practical applications such as electronics, optoelectronics and photonics. The best-known conjugated polymers are those with extended π -system and involving alternating C=C and C-C bonds, such as polyacetylene, poly(p-phenylene) and poly(p-phenylenevinylene). A class of the particularly attractive conjugated polymers are the aromatic polyazomethines or Schiff base polymers. Aromatic polyazomethines, being conjugated polymers with the extended π -system, have alternately CH=N group and benzene ring in the main chain [5-13].

In the present work, the 1,4-phenylenemethylenenitrilo-1,4-phenylenenitrilomethylene (PPI) thin films prepared by chemical vapor deposition (CVD) [14,15,16] have been examined. The aim

of our paper is an attempt to describe the changes in surface morphology and roughness of PPI films, by the atomic force microscope and scanning electron microscope as dependent on conditions of the polymer film preparation.

2. Materials and methodology

Thin films of PPI have been prepared by chemical vapor deposition method based on polycondensation of p-phenylene diamine (PPDA) and therephthal aldehyde TPA. This technique can be applied only while polymerization is going through condensation as the only product that is removed from the reaction volume is a low weight molecular material. In case of polyazomethines this is one water molecule, removing of which from the reaction volume being responsible for the reaction progression [17,18].

2.1. PPI thin film preparation

Polyazomethine thin films were prepared by polycondensation of PPDA and TPA following the reaction as below (Fig. 2). Both monomers, TPA and PPDA were purchased from ALDRICH. Thin films of polyazomethine PPI were prepared using low-temperature chemical vapor deposition (LCVD) method. PPI thin films were prepared at TPA temperature of 60°C and the PPDA temperature of 80°C during 2 min under various argon streams. Deposition process parameters are presented in Table 1.

2.2. Experimental

Polyazomethine thin layers were deposited onto BK7 glass. The thickness of prepared films was about 100-300 nm depending on flow rate of gas transport.

The changes in surface topography was observed by the atomic force microscope AFM [19,20] working in the contact mode and scanning electron microscope SEM. The results of roughness have been prepared in the software WSxM NanoTec Spanish company.

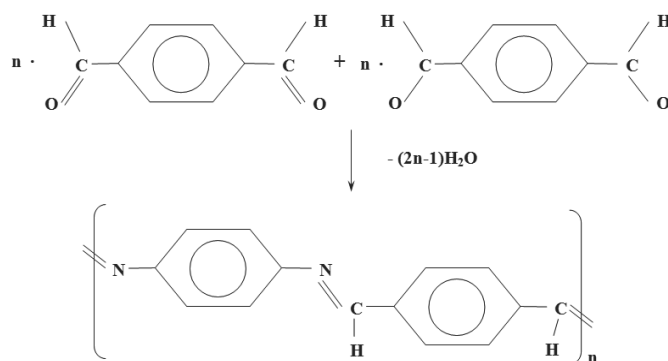


Fig. 2. Scheme of polyazomethine PPI polycondensation

3. Results and discussion

Topography of the surface of each PPI thin film prepared under various technological conditions are shown in Figures 3-7. The A thin film whose surface topography was obtained under a small stream of transport gas equal to 0.05 [Tr·l/s] is shown in Fig. 3. The A thin film reveals a uniform granular structure without any precipitates. The 3D view shows that there are numerous smaller surface undulations which may be indicative of its high roughness.

Fig. 4 shows the granular surface of the B thin film. The increase of transport gas from 0.05 to 0.15 [Tr·l/s] caused the appearance of precipitates of different shapes. Also in the 3D picture see undulations in the areas between the precipitates.

Fig. 5 shows that the increase of flux to a value of 0.4 [Tr·l/s] was smoothed the surface between the precipitates. We may even notice that the precipitates in the C thin film are not as numerous as in the B thin film. The 3D view shows that the red square marked precipitate it is a structure growing perpendicular to the background.

Fig. 6 shows the granular structure of the D thin film. The increase in the value of a stream to 1 [Tr·l/s] caused a decrease precipitation, which adopted the form of granules, the diameter of ~ 0.5 μm.

Topography of the surface E thin film was obtained by the large stream of transport gas, equal to 3 [Tr·l/s], is shown in

Fig. 7. The E thin film has a granular structure. Threefold increase in flow caused the large precipitates of excess length of ~ 1 μm.

The AFM and SEM images of the A and E thin films surfaces are shown in Figures 8-10. The AFM and SEM images are very similar and present the granular structure of the A thin film, the granules have a diameter of ~ 0.20 μm.

Fig. 8 b shows the effect of electron beam impact on the sample. In the central part of the image made at a magnification of 40 000 times the square is visible trace of action on the PPI thin film of electron beam at a magnification of 100 000 times. This is because that the area observations at a magnification of 40 000 times is much larger than the 100 000 times magnification. Seen following is the result of thermal impact of the electron beam with the surface of the polymer material with low thermal conductivity. While examining as prepared PPI thin films by SEM, electrifying their surfaces has appeared to be an obstacle difficult to overcome. This effect is shown in Fig. 9 where there is a lack of contrast and image blur. Therefore it was decided to cover PPI thin film surface with a layer of gold. Thin layer of gold does not change the morphology of the surface layer and as a metallic layer prevents the accumulation of static surface.

In Fig. 10 see the comparison of E thin film images, obtained by atomic force microscope and scanning electron microscope. In Fig. 10b, although deposited gold can still be seen on the outskirts of large precipitates glowing effects, and poor image contrast, as a consequence of electrification of the material. Although this, the images obtained on both microscopes are similar.

Table 1.
Deposition process parameters

Thin film	TPA temperature [°C]	PPDA temperature [°C]	Ar flow rate [Tr·l/s]	Deposition time [min]
A	60	80	0.05	2
B			0.15	
C			0.4	
D			1	
E			3	

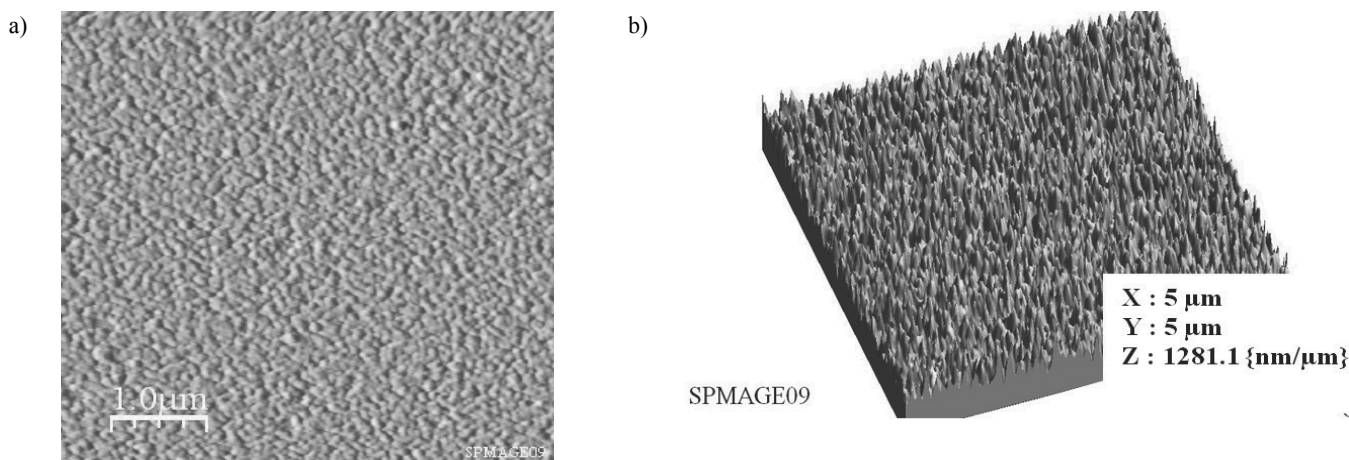


Fig. 3. AFM images of A thin film: a) 2D view, b) 3D view

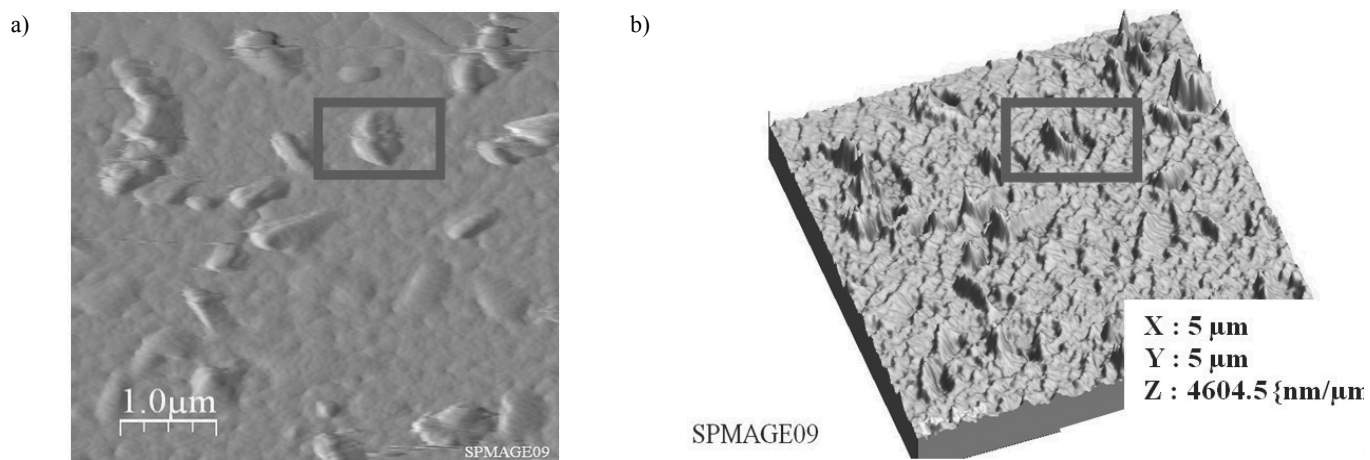


Fig. 4. AFM images of B thin film: a) 2D view, b) 3D view

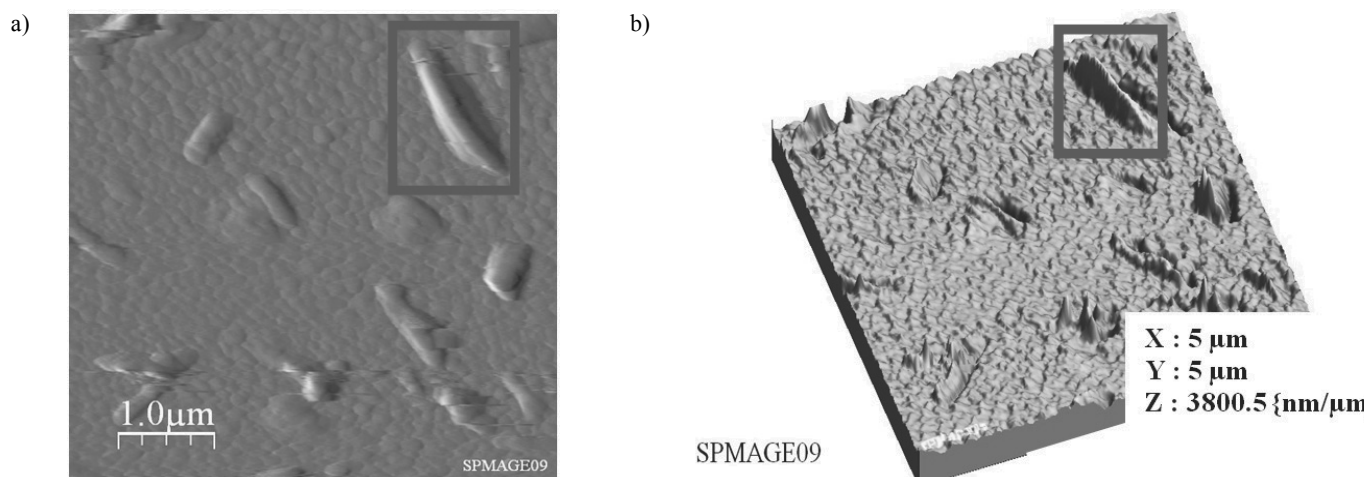


Fig. 5. AFM images of C thin film: a) 2D view, b) 3D view

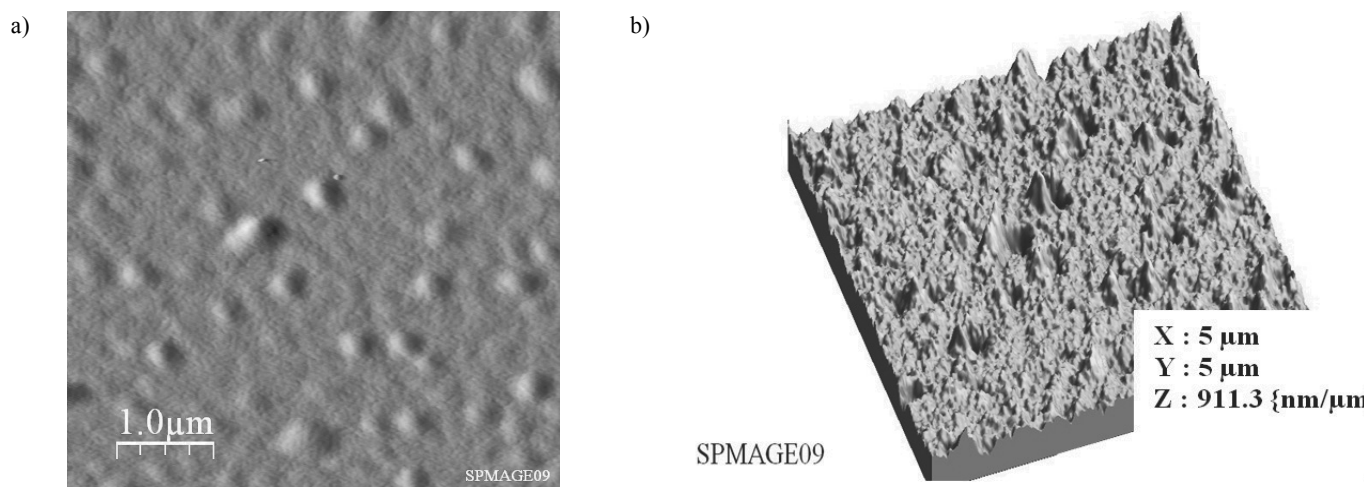


Fig. 6. AFM images of D thin film: a) 2D view, b) 3D view

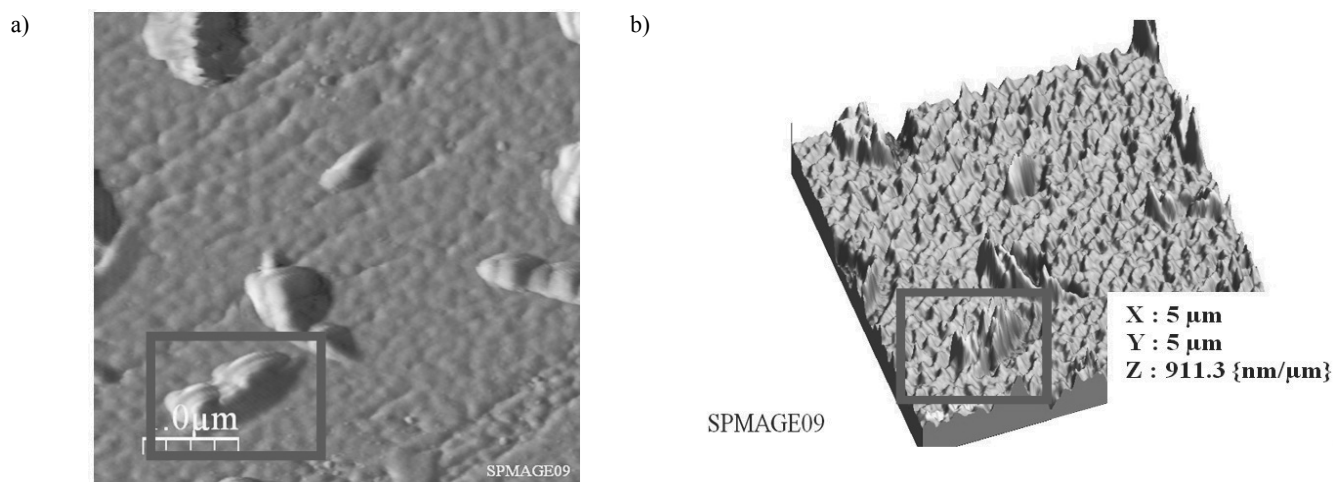


Fig. 7. AFM images of E thin film: a) 2D view, b) 3D view

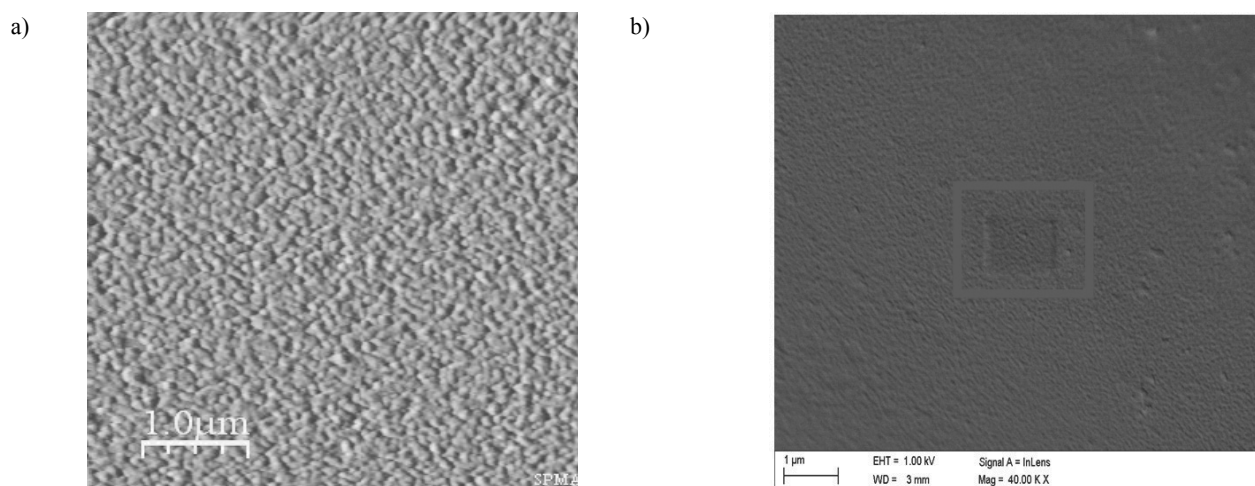


Fig. 8. Comparison of E thin film images: a) AFM, b) SEM

Table 2.

Roughness parameters calculated in WSxM

Parameters/Thin films	A	B	C	D	E
RMS [nm]	142.425	232.510	173.742	64.6379	261.531
Ra [nm]	113.925	142.360	94.311	37.861	157.589
Max. elevation [nm]	685.178	2697	2447.51	551.579	1772.470

Figures 11-15 presents an analysis of the roughness each thin layer carried out in the WSxM program. The roughness was characterized by calculating the RMS roughness parameter and presenting the histogram.

Fig. 11 shows the histogram of the A thin film - the distribution of inequalities of its surface. The shape of the histogram and the result obtained RMS, equal to 142.425 nm, are in conformity with the conclusions drawn from the observation of

surface topography. The histogram of B thin film, shown in Fig. 12, we can see a big precipitates, exceeding even the amount of 2.5 μm, characterized by a low prevalence. The RMS roughness coefficient of at 232.510 nm, indicates that the precipitates of the data for a large proportion of surface irregularities.

Histogram of the C thin film as shown in Fig. 13 shows that in the layer C thin film are less precipitates and less frequently than

in B thin film, which is reflected in the value of $RMS = 173.42$ nm, lower than in the case of B thin film.

Fig. 14 shows the histogram of the D thin film - distribution of irregularities of its surface. The D thin film is characterized by the lowest coefficient of roughness $RMS = 64.6379$ nm layers of the PPI investigated. This interacts to a lower incidence of irregularities and their size.

The E thin film has the highest coefficient of roughness $RMS = 261.531$ nm. The histogram shown in Fig. 15 shows that the incidence of high precipitation is too high which has the greatest impact on such a high surface roughness.

These results are presented in Table 2.

Table 3.

Roughness parameters of D thin film

Thin film /Parameters	RMS [nm]	Ra [nm]	Max. elevation [nm]
D	64.6379	37.861	551.579

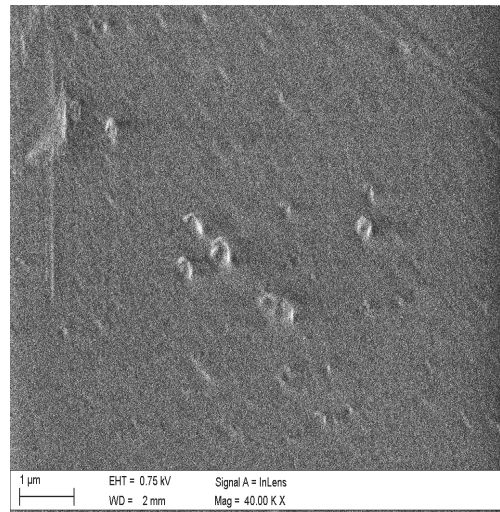


Fig. 9. The effects of electrification of the material

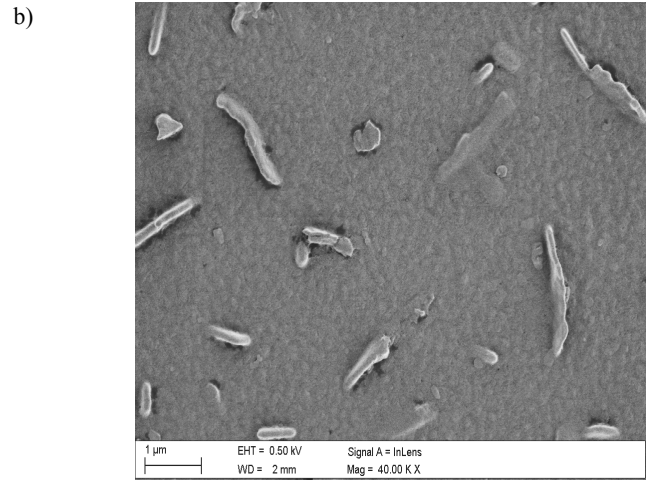
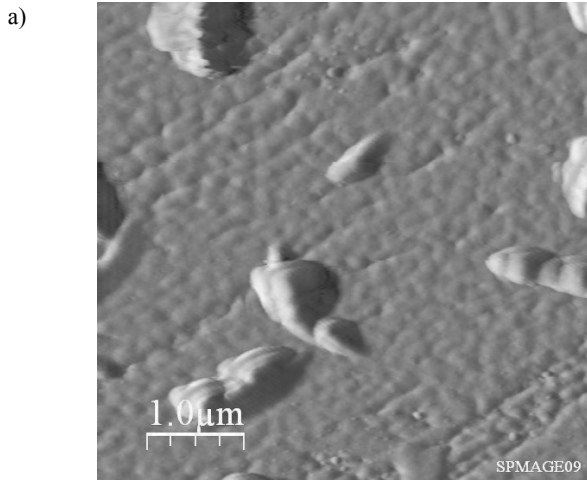


Fig. 10. Images surface topography E thin film: a) AFM, b) SEM

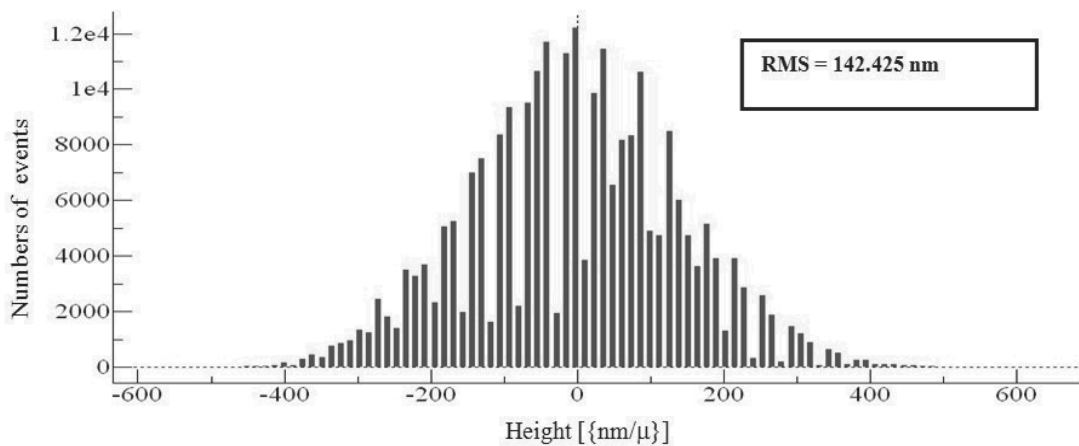


Fig. 11. The A thin film histogram of occurrence of height

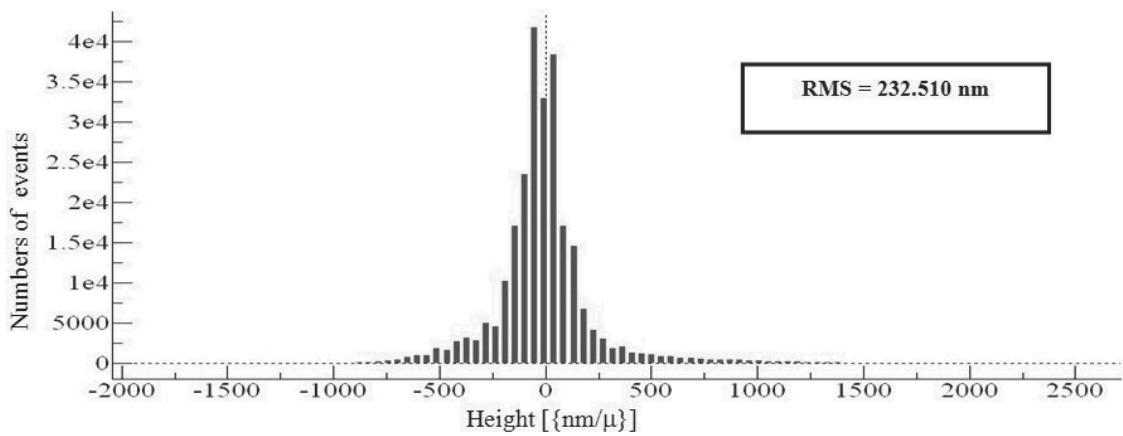


Fig. 12. The B thin film histogram of occurrence of height

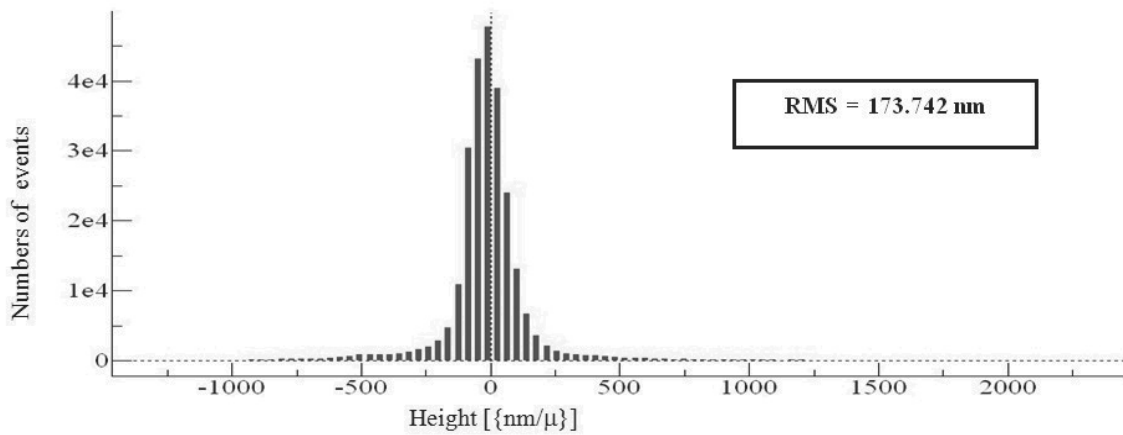


Fig. 13. The C thin film histogram of occurrence of height

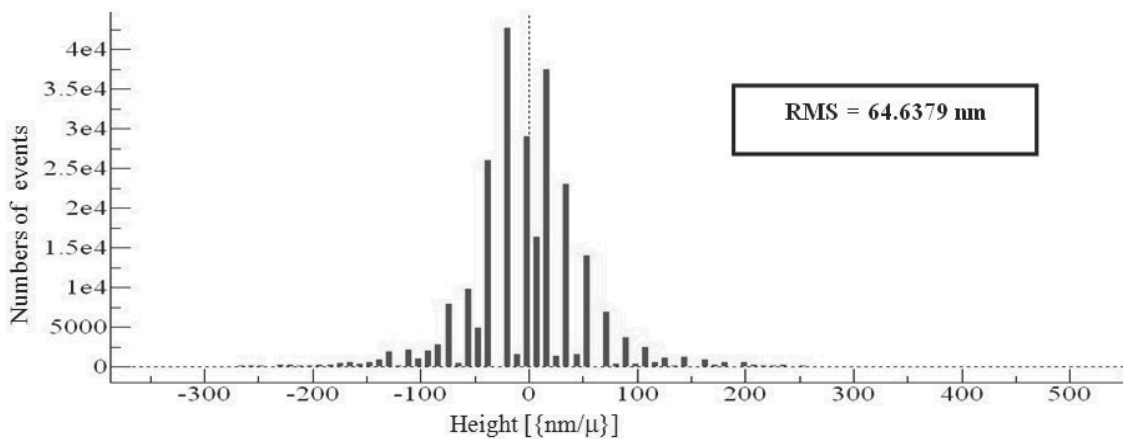


Fig. 14. The D thin film histogram of occurrence of height

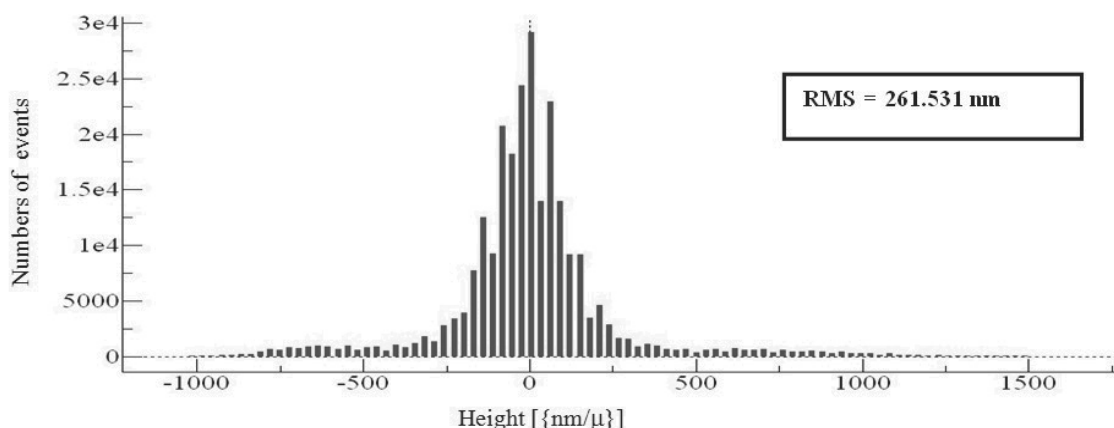


Fig. 15. The E thin film histogram of occurrence of height

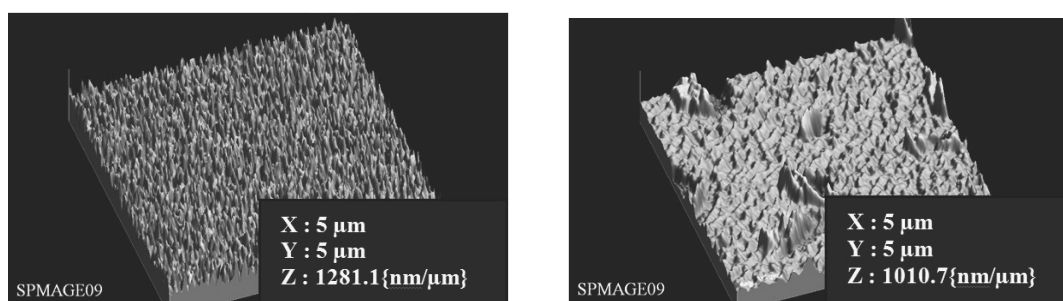


Fig. 16. AFM images comparison of thin film A and B

4. Conclusions

PPI thin films were prepared at aldehyde temperature of 60°C and the amines temperature of 80°C during 2 min under various gas streams. On the basis of the results can be concluded that at low carrier gas flow equal to 0.05 [Tr-l/s] layer does not have any more precipitation, but has a number of smaller inequalities. With increasing carrier gas flow there are numerous, large separation of the structures that are growing perpendicular to substrate. If, however, ignore them in these deliberations, the layer of such a characteristic in the distribution of uniformly than at low carrier gas stream. Comparison of structures obtained at low and high transport gas stream is shown in Fig. 16.

Comparing the roughness parameters preferably fared D thin film deposited by a stream of carrier gas of 1 [Tr-l/s]. The D thin film roughness parameters are presented in Table 3.

Acknowledgements

Marek Szindler is a holder of scholarship from project POKL.04.01.01-00-003/09-00 entitled „Opening and develop-

ment of engineering and PhD studies in the field of nanotechnology and materials science” (INFONANO), co-funded by the European Union from financial resources of European Social Fund and headed by Prof. L.A. Dobrzański.



HUMAN CAPITAL
NATIONAL COHESION STRATEGY



References

- [1] A. Terje Skothei, J. Reynolds, Handbook of Conducting Polymers, 2007.
- [2] The Nobel Prize in Chemistry 2000, web site http://nobelprize.org/nobel_prizes/chemistry/laureates/2000/public.html.
- [3] C. Pratt, Conducting Polymers, web site <http://homepage.dtn.ntl.com/colinpratt/cpoly.htm>.
- [4] Conductive polymers BBC group report, web site <http://www.bccresearch.com/report/PLS043B.html>.
- [5] B. Hajduk, J. Weszka, V. Cozan, B. Kaczmarczyk, B. Jarzabek, M. Domański, Optical properties of polyazomethine with oxygen atom in the backbone,

- Archives of Materials Science and Engineering 32/2 (2008) 85-88.
- [6] J. Wieszka, M. Domański, B. Jarzabek, J. Jurusik, J. Cisowski, A. Burian, Influence of technological conditions on electronic transitions in chemical vapor deposited poly(azomethine) thin films, *Thin Solid Films* 516 (2008) 3098-3104.
- [7] B. Hajduk, J. Wieszka, B. Jarzabek, J. Jurusik, M. Domański, Physical properties of polyazomethine thin films doped with iodine, *Journal of Achievements in Materials and Manufacturing Engineering* 24/1 (2007) 67-70.
- [8] B. Jarzabek, J. Wieszka, M. Domański, J. Jurusik, J. Cisowski, Optical studies of aromatic polyazomethine thin films, *Journal of Non-Crystalline Solids* 354 (2008) 856-862.
- [9] B. Jarzabek, J. Wieszka, M. Domański, J. Cisowski, Optical properties of amorphous polyazomethine thin films, *Journal of Non-Crystalline Solids* 352 (2006) 1660-1662.
- [10] L.A. Dobrzański, Engineering materials and materials design. Fundamentals of materials science and physical metallurgy, WNT, Warsaw-Gliwice, 2006 (in Polish).
- [11] B. Hajduk, J. Wieszka, J. Jurusik, Influence of LCVD technological parameters on properties of polyazomethine thin films, *Journal of Achievements in Materials and Manufacturing Engineering* 36/1 (2009) 41-48.
- [12] W. Łużny, E. Stochmal-Pomarzańska, A. Proń, Structural properties of selected poly(azomethines), *Polymer* 40 (1999) 6611-6614.
- [13] M. Palewicz, A. Iwan, M. Sibinski, A. Sikora, B. Mazurek, Organic photovoltaic devices based on polyazomethine and fullerene, *Energy Procedia* 3 (2011) 84-91.
- [14] L.A. Dobrzański, K. Lukaszewicz, D. Pakuła, J. Mikuła, Corrosion resistance of multilayer and gradient coatings deposited by PVD and CVD techniques, *Archives of Materials Science and Engineering* 28/1 (2007) 12-18.
- [15] D. Pakuła, L.A. Dobrzański, Investigation of the structure and properties of PVD and CVD coating deposited on the Si₃N₄ nitride ceramics, *Journal of Achievements in Materials and Manufacturing Engineering* 24/2 (2007) 79-82.
- [16] L.A. Dobrzański, S. Skrzypek, D. Pakuła, J. Mikuła, A. Křiž, Influence of the PVD and CVD technologies on the residual macrostresses and functional properties of the coated tool ceramics, *Journal of Achievements in Materials and Manufacturing Engineering* 35/2 (2010) 162-168.
- [17] J. Wieszka, B. Hajduk, M. Domański, M. Chwastek, J. Jurusik, B. Jarzabek, H. Bednarski, P. Jarka, Tailoring electronic structure of polyazomethines thin films, *Journal of Achievements in Materials and Manufacturing Engineering* 42 (2010) 180-187.
- [18] J. Wieszka, H. Bednarski, M. Domański, Electronic structure of poly(azomethine) thin films, *Journal of Chemical Physics* 131/2 (2009) 02490-1-02490-9.
- [19] W. Kwaśny, L.A. Dobrzański, M. Król, J. Mikuła, Fractal and multifractal characteristics of PVD coatings, *Journal of Achievements in Materials and Manufacturing Engineering* 24/2 (2007) 159-162.
- [20] W. Kwaśny, W. Sitek, L.A. Dobrzański, Modelling of properties of PVD coating using neural networks, *Journal of Achievements in Materials and Manufacturing Engineering* 24/2 (2007) 163-166.